Solvent effects to compute UV-vis spectra for ionic metal complexes

S. Boumendil, J.P. Cornard, M. Sekkal-Rahal, A. Moncomble

Solvent effects to compute UV-vis spectra for ionic metal complexes

Sonia Boumendil,[1,2] Jean-Paul Cornard,[1] Majda Sekkal-Rahal,[2] Aurélien Moncomble[1*]

1) LASIR, UMR CNRS 8516, Université de Lille – Sciences et Technologies, 59655 Villeneuve d'Ascq Cedex, France

mail: aurelien.moncomble@univ-lille1.fr; tel: +33 3 20 43 49 14

2) Laboratoire de Microscopie, Microanalyse de la matière et Spectroscopie Moléculaire, Université Djilali Liabès, B.P 89, Sidi Bel Abbès 22000, Algeria

Graphical abstract

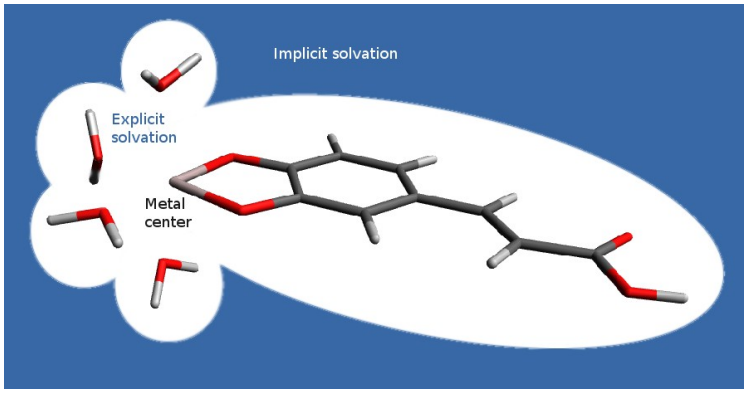

Abstract

The correct representation of the solvent is a crucial issue for the computation of molecular properties in solution, especially UV-vis spectra.

This article shows that for mainly ionic complexes involving intra-ligand electronic transitions, the use of a hybrid model (microsolvation and PCM) leads to a good reproduction of the experimental electronic spectra. The use of smaller molecules (water instead of methanol) in the first coordination sphere did not change the optical absorption computation, saving by this way computation time. A tentative explanation based on the nature of the solvent—metal cation bonds is then presented.

Keywords: Complexes; DFT; Solvation; TD-DFT; UV-visible spectra

Cartesian coordinates for species labeled CA and CA-2H and complexes 1, 2, 3 and 4 (2 flavours) are reported in SI.

1. Introduction

Solvent description is a crucial point for the good reproduction of many physical or chemical properties with quantum-chemistry-based methods. Among them, solubility[1], pK_A[2] and redox potential[3] computations have been deeply investigated due to the explicit involvement of the solvent. Nevertheless, many other properties are influenced by the solvent and need a careful representation of its properties. It is especially the case of spectroscopic properties such as UV-vis absorption. Indeed, the solvatochromism is quite important on many molecules that prevents one from neglecting the solvent in this case.

The computation of UV-vis spectra has drawn attention in the last decades and many methods are now well-suited to reproduce and predict the absorption properties of molecules[4]. These methods are crudely grouped in two categories: wave-function or electron-density based. The former category is represented by methods such as CIS, CASSCF, CASPT2[5], EOM-CC[6], CC-LRT[7], SAC-CI[8] or ADC(2)[9]. The latter one is mainly represented by TD-DFT methods[10]. TD-DFT methods have been shown to give accuracy comparable to post-Hartree-Fock methods with a suitable functional[11], it is therefore often regarded as a good compromise between accuracy and CPU time for metal complexes[12,13]. Then, this article will be limited to the application of TD-DFT to compute electronic excitations.

Several models are possible for the solvent in quantum chemistry and most of them are applicable to TD-DFT computations. This issue has been deeply studied by many groups on several molecules families. First the solvent can be represented by a continuum[14]. In this case, no individual solvent molecule appears, but their bulk properties are replaced by some macroscopic (dielectric constant for instance) and microscopic (solvent radius for instance) quantities. The formalism to use this model with TD-DFT is now developed and implemented in some computation codes[15] with some variants whose influence has been studied in details[16–18]. Second the solvent molecules can be represented individually, that is generally processed by the use of molecular dynamics based

methods: many examples are now given were geometries are obtained by any computational method; some snapshots are then extracted and the low-lying excitations are computed and summed up to obtain a spectrum accounting for a large subset of the possible conformations[19,20]. These two approaches possess both strengths and weakness. The explicit representation is a better microscopic representation of the system but taking into account enough solvent molecules can be quite CPU-expensive. The computation time needed by the dynamics can be diminished by the use of molecular mechanics or QM/MM methods. The implicit representation is faster as less electrons are taken into account, but the parameters chosen to represent the solvent and the variety of implementations is wide that can lead to more empiricism in its application.

Another approach is to mix explicit and implicit methods to try to obtain advantages from both methods. A first way to apply this method is from the explicit method: once the structures obtained with the explicit solvent obtained, molecular structures are extracted but the solvent molecules are removed and replaced (without geometry re-optimization) by an implicit solvent to compute the excitations[21], saving by this way CPU time in the last step. A second way roots in the implicit method: instead to take account of each solvent molecule, only a few chosen ones are added on the most important part of the molecules (microsolvation); around this structure, a continuum model is added to fully account for the solvent[22,23]. This last semi-implicit method is chemically appealing: the CPU time is reduced in comparison with a fully explicit model while the significant microscopic parameters are kept. However, it needs a good knowledge of the studied system to avoid to skip some important molecules or to add non useful ones that would lengthen computations without increasing the precision of obtained results[24–26].

The purpose of this article is to advocate that in the case of ionic metal complexes, explicit solvent molecules need to be added to correctly account for the solvent influence on UV-vis parameters. For metal cations whose solvation sphere is non-isotropic, such as copper(II) or lead(II), some elements to prove it have yet been given in our previous works[27] but in the case of more symmetrical

coordination sphere, the proof is still needed. This will be illustrated by the study of an example: the complex (CA-Al) formed by the complexation of Al^{III} cation with caffeic acid (CA) (see Figure 1) in methanol solution. CA is a naturally occurring molecule released by some plants to form complexes with nutriments and stabilize them in a oxidation state assimilable by plants[28]. Therefore, its complexation is a subject of importance that has been studied in our team and the structure of its complex with Al^{III} cation (chelation to the fully-deprotonated catechol group) has been determined by an approach comparing measured and computed UV-vis data[29,30]. Then, we focused only on the nature of the solvent model used.

The importance of adding some solvent molecules will be emphasized by showing that it leads to a good reproduction of the experimental data that a purely implicit solvent model cannot achieve. Then, the possibility to replace the solvent molecules by smaller ones will be emphasized. Last, a tentative explanation of these features will be proposed based on the nature of the bonds implied in the studied complex.

2. Computational details

All calculations were carried out with the Gaussian 09 set of programs[31]. DFT-based methods, including its time-dependent version (TD-DFT) were used throughout. More specifically, B3LYP global hybrid functional[32–35] was used due to its ability to compute absorption properties in the UV-vis domain[11]. The 6-31+G** basis set was used to represent all atoms[36–38]. Structural optimizations were processed using standard algorithms without any symmetry constraint. The nature of minima was checked by subsequent vibrational analysis. TD-DFT formalism was used in the adiabatic approximation to compute excitation energies and associated oscillators strengths. The lowest excited states were taken into account to compute vertical excitation energies (the number of states taken into account was chosen for each complex to obtain all excitations below 200 nm (6.20 eV)).

The model for the solvent is studied below, but when a continuum represents the solvent (methanol), PCM, as implemented in Gaussian with the internal parameters for methanol, is used[14,39]. More precisely, the Integral Equation Formalism (IEF) was used in the linear response approach. Some tests (not detailed in this letter) have been performed with state-specific solvation, but no significant change was observed on the studied systems. The study reported here focused on absorption properties so non-equilibrium solvation was used throughout.

Atoms-in-molecules (AIM) computations[40] were carried out to give some insight about the bond nature in the studied complexes. Bond critical points (BCPs) and ring critical points (RCPs) were located, and local and integrated properties were computed using the AIMAll software[41].

3. Presentation of the models used

The absorption electronic spectrum of CA-Al has been recorded in methanol solution[29] so the best representation of this solvent to reproduce the experimental results is the purpose of this letter. Several models involving microsolvation and/or continuum model were therefore used. Starting from the simplest model (**1**, no solvation of any kind), two directions were explored. The addition of a continuum (characterized, among other parameters, by $\varepsilon = 32.613$ for methanol) leads to model **2** while the addition of explicit molecules (methanol) around the complex leads to model **3**. When these two approaches are mixed, a fourth model (labeled **4**) is obtained. In each case, optimizations have been carried out and electronic transitions were computed. To fulfill a good understanding of the underlying phenomenons, two unusual models were introduced from **3** and **4** by removing the explicit solvent molecules and recomputing the electronic transitions without re-optimizing the structure of the complexes. These last two models are labeled **3'** and **4'**. The main characteristics of those models are recalled in the synthetic Table 1.

Models involving explicit molecules of methanol (**3** and **4**) imply a choice on the position of the solvent around the molecules. Preliminary studies on CA have been carried out. Several structural hypotheses were computed involving interaction between solvent and the two main functional groups located on CA (catechol and carboxylic acid) and the electronic transitions were computed. When comparing the computed value for the lowest-energy electronic transition with the experimental value obtained in methanol (314 nm, 3.95 eV), the best compromise between accuracy and precision of the computed transition was obtained using the continuum model only whose result (324 nm, 3.83 eV) is in line with the accuracy of TD-DFT methods, while adding solvent molecules did not improve the result or even deteriorate it (for instance, the addition of two molecules on the catechol and two on the carboxylic acid gives a computed value of 337 nm (3.68 eV) for the equivalent transition). This has been confirmed for CA-Al by some computations carried out with more explicit molecules: additions on other functional groups did not lead to any improvement

while addition in the second coordination sphere of the cation results in delicate structural optimizations without accuracy benefit. Therefore, in the following, the explicit interaction between the solvent and CA-Al in models **3** and **4** will only be considered by the interaction of the Al^{III} cation and methanol molecules.

4. Study of these different models for CA-Al

4.1. Geometrical investigation

The six models have been applied to the study of CA-Al and structural optimizations were carried out. Some significant geometrical parameters for CA, CA-2H (a formal structure where the two protons of catechol have been removed from CA) and the six models of complexes are reported in Table 2. The structure of models **2** and **4** are depicted in Figure 2.

Some structural parameters appear to be quite disturbing in models **1** and **2**. First, the metal cation is not in the same plane as the ligand as illustrated by the value of Al-O3'-C3'-C4' and Al-O4'-C4'-C3' dihedral angles. This odd result should be explained by an interaction between the aromatic moiety and the cation that has not been quantified in this work. Second, the aromatic ring is strongly affected and its aromaticity seems to be lowered that should be evidenced by some structural (standard deviation of the six C—C bond lengths of the benzene ring) or electronic (electron density (ρ) and total electron density (H) at the RCP[42] and Para Delocalization Index (PDI) [43]) parameters devoted to the evaluation of aromaticity. These values (reported in Table 2) are consistent with a higher aromaticity of CA, **3** and **4** than **1** and **2**. This aspect is confirmed by the value of some dihedral angles between four carbons of the aromatic ring (not reported in Table 2 for the sake of clarity) that are different from 0° in **1** and **2** while the equivalent values are very close to 0° in the three other cases. This is especially significant when considering the C3'—C4' bond whose lengthening is large in **1** and **2**, associated with a shortening of C3'—O3' and C4'—O4' bonds, that evokes the structure of a dianion obtained from the full deprotonation of the catechol. Indeed, these features are recovered and even amplified when the structure CA-2H is computed. Therefore, models **1** and **2** treat the CA-Al complex by a bare interaction between a cation Al^{III} associated with the CA-2H dianion (that is confirmed by the quite long bonds between O3' and O4' in one hand and Al in the other hand), while models **3** and **4** seem to imply a more important rearrangement with respect to CA-2H.

To check which model is closer from the actual CA-Al, the electronic transitions were computed for these six models.

4.2. Electronic transitions

The use of TD-DFT methods leads to the computation of the transitions depicted in Figure 3 along with the experimental spectrum. The most important transitions (oscillator strengths above 0.05) are reported in Table 3.

The first conclusion to be drawn from this comparison is that using a fully implicit model for the representation of CA-Al (**2**) did not lead to significant improvement when compared with no solvation (**1**). Therefore, beyond the odd structures obtained (see section 4.1), the electronic transitions are badly reproduced by this sole continuum model. The addition of explicit solvent molecules eliminates the transitions computed at very low energies (as illustrated by the modifications from **1** and **2** to **3** and **4** respectively).

As expected, the sole consideration of the solvent molecules around the cation is not sufficient. Indeed, for the lowest band measured, model **3** presents a significant blue shift (70 nm (0.78 eV)) when compared with the experimental data while model **4** is shifted by only 17 nm (0.16 eV), in line with the accuracy of TD-DFT methods. The same trend is observed for the other transitions.

These results illustrate that explicit molecules of solvent are needed around the cation. However, the solvent need to be taken into account all around the molecule but implicit model is sufficient to reproduce the main features of UV-vis spectra whenever the solvent does not play the role of a ligand.

Two models were introduced earlier to give more insight. Indeed, the addition of explicit solvent molecules appears in two different aspects. First, it implies strong structural constraints (discussed in part 4.1). Second, it should have an influence on the computation of electronic transitions from this optimized structures. Therefore, this two effects were separated by the introduction of models **3'** and **4'** where the structure is optimized with explicit solvent molecules around the cation that are removed to compute the electronic transitions. The results reported in Table 3 and Figure 3 illustrate two different effects. First, non-physical electron transitions are computed in **3'** and **4'** as in **1** and **2**

on the wavelength range above 500 nm. Their presence should be assigned to the fact that these structures are not rigorously energetic minima: **3'** and **4'** are not optimized and **1** and **2** seems to involve a quite unsatisfactory consideration of the solvent. Second, the comparison of the most significant (i.e. excluding transitions without physical sense) low-energy transition from **2** (315.1 nm) to **4** (352.8 nm) via **4'** (323.0 nm) illustrates that the main effect of explicit solvation on the values of computed transitions on this kind of complexes directly roots in their computations (**4'** to **4**) and is not a side effect of a worse geometry (**2** to **4'**).

4.3. Simplification: utilization of water molecules

Once established that model **4** is the most able to reproduce the features of the experimental spectra, and so certainly the closest of the "true" structure of the complex, we attempted to simplify it and to limit computation time. Previous sections show that removing explicit molecules is not a solution so we tried to use smaller molecules that resemble methanol. As the bond between aluminum and solvent appears to be ionic, it was chosen to replace methanol by water: this simplification appears quite rough but will be justified in section 5 by the study of bonding in the complex.

The objective to decrease the computation time is achieved in two ways: the number of atoms (and then of electrons) is decreased, saving time for each SCF cycle (in this case, 144 electrons are present instead of 176, that is a theoretical reduction of the computation time for each cycle of nearly 45% assuming a N^3 scaling), and water molecules bear less degree of freedom that shorten the structural optimization procedure.

The electronic transitions for three flavors of model **4** are then reported in Table 4. It appears clearly that the influence of the precise nature of the explicit molecules is negligible. In the case of study, the influence of the implicit solvent is also quite small, even if more important, but it is quite questionable to change this parameter as no computation time is saved by the alteration of this parameter. Therefore, the use of explicit water molecules with an implicit methanol continuum appears as a good compromise.

Moreover, pH variations can be taken into account by replacing some water molecules by hydroxide anions in the coordination sphere of the metal: the more alkaline the medium is, the more anion will be introduced. Some works in our group have yet shown the efficiency of this methodology[27,44].

5. Study of the nature of bonds in complexes

To challenge the hypothesis presented in section 4.3 about the nature of the bonds involved, we proceeded to a detailed study of the nature of bonds around Al^{III}. In this section, a particular attention is given to the effect of explicit molecules on the structure of the complexes, so only the models involving methanol as an implicit solvent are used: **2** without any explicit molecule, **4** that contains methanol molecules and its variation with water molecules. Some AIM quantities for these bonds are reported in Table 5.

All the studied bonds present a strong ionic character, revealed by the low ρ(BCP) value, the large positive value of Δρ(BCP) and the very small (but positive) value of the total electronic energy density for each BCP (H(BCP))[45]. These results are confirmed by the computed values for the ratio -G(BCP)/V(BCP) (where G is the kinetic electronic energy density and V the potential energy density) that is higher than 1, implying purely non-covalent interactions[46].

The two flavors of model **4** appear to be indistinguishable, in line with results previously presented, that confirms the ability of water molecules to correctly represent the first solvation sphere instead of methanol. These molecules are loosely bound to the metal center, that is illustrated by the low value of all quantities at the BCP, including ρ(BCP). Interestingly, the values of the delocalization index (δ) are also very low, confirming the low interaction between the solvent and the aluminum[47,48].

The most remarkable difference between **2** and the two flavors of **4** is the value of the AIM charge on the aluminum atom (1.50 for Al in **2** and 2.57 in both variations of **4**). This very large difference is confirmed by the computation of another kind of charges (NPA charges: 1.32 for Al in **2** while 2.04 and 1.97 are obtained for the two variations of **4**). Therefore, the absence of explicit molecules of solvent appears to decrease the ionic character of the Al—catechol bonds. The comparison between the value of Δρ(BCP) and of G(BCP) confirms this hypothesis: the values computed are lower in **2** than in **4**. Moreover, the delocalization index is twice as large in **2** as in **4**. It appears that

the aluminum cation is not solvated enough in **2** by the implicit solvent, and attracts the electron density from its ligand, leading to a decrease of its charge and of the ionic character of metal-ligand bonds, and to the large deformation reported in section 4.1. The explicit molecules added in **4** are solvent molecules that play the role of ligands, leading to an interaction with the aluminum atom, the electron density of the ligand should then stay on the ligand instead of be involved in the bond with the cation.

A last kind of computation was carried out to reinforce this interpretation. The structural optimization and the computation of the transitions for the two flavors of **4** were realized with the use for the aluminum atom of the Hay-Wadt ECP[49] that contains the ten inner electrons. No valency basis function was added to prevent the localization of more electrons on Al^{III} (that was confirmed by the Mulliken charge for this atom that rigorously equals +3 in this computation (the use of the Mulliken charge is on purpose, despite some well-known weaknesses[50], because a wave-function scheme is needed to confirm the absence of valence electrons on Al)). When the computed transition energies are compared with those reported in Table 4, only one presents a shift of 0.05 eV (7 nm in this wavelength domain), the other shifts being significantly below this value. This very good agreement between these computations confirms the non-involvement of valency basis functions of aluminum and thus the ionic character of the Al—O bonds in this molecule.

Conclusion

A model has been presented in this work to compute electronic transitions in the case of metallic complexes in a coordinating solvent where the metal-ligand and metal-solvent interactions are mainly ionic. Internal parameters of a widespread software are used without any modification and only the nature of the solvation sphere of the cation is needed, and is predictable by computations.

The main characteristics of this model are:

- a first coordination sphere explicitly reproduced by a simplified molecule (water instead of methanol) around the metal center;
- no necessity to add explicit molecules anywhere else around the ligand;
- an implicit solvent is added around this complex by the means of the PCM formalism.

A fast and accurate reproduction of optical transitions is achieved and leads to significantly better results than the other presented protocols. A tentative rationalization of this procedure is given, based on the nature of the bonds involved and electron displacement in the molecule depending on the solvation model.

Acknowledgments

This work was granted access to the HPC resources of CINES and IDRIS under the allocations 2014086933 and 2015086933 made by GENCI (Grand Equipement National de Calcul Intensif). We also thank the CRI (Centre de Ressources Informatiques) of the Université de Lille for providing computing time for part of the theoretical calculations.

SB thanks the Ministère de l'Enseignement Supérieur et de la Recherche Scientifique (MESRS, Algeria) for a grant.

References

[1] N.E. Jackson, L.X. Chen, M.A. Ratner, Solubility of Nonelectrolytes: A First-Principles Computational Approach, J. Phys. Chem. B. 118 (2014) 5194–5202. doi:10.1021/jp5024197.

[2] G. Shields, P. Seybold, Computational Approaches for the Prediction of pKa Values, CRC Press, 2013. http://www.crcnetbase.com/doi/book/10.1201/b16128 (accessed August 27, 2014).

[3] A.V. Marenich, J. Ho, M.L. Coote, C.J. Cramer, D.G. Truhlar, Computational electrochemistry: prediction of liquid-phase reduction potentials, Phys. Chem. Chem. Phys. 16 (2014) 15068. doi:10.1039/c4cp01572j.

[4] M. Olivucci, ed., Computational photochemistry, 1st ed, Elsevier, Amsterdam ; Boston, 2005.

[5] K. Andersson, P.A. Malmqvist, B.O. Roos, A.J. Sadlej, K. Wolinski, Second-order perturbation theory with a CASSCF reference function, J. Phys. Chem. 94 (1990) 5483–5488. doi:10.1021/j100377a012.

[6] J. Geertsen, M. Rittby, R.J. Bartlett, The equation-of-motion coupled-cluster method: Excitation energies of Be and CO, Chem. Phys. Lett. 164 (1989) 57–62. doi:10.1016/0009-2614(89)85202-9.

[7] D. Mukherjee, P.K. Mukherjee, A response-function approach to the direct calculation of the transition-energy in a multiple-cluster expansion formalism, Chem. Phys. 39 (1979) 325–335. doi:10.1016/0301-0104(79)80153-6.

[8] H. Nakatsuji, Cluster expansion of the wavefunction. Electron correlations in ground and excited states by SAC (symmetry-adapted-cluster) and SAC CI theories, Chem. Phys. Lett. 67 (1979) 329–333. doi:10.1016/0009-2614(79)85172-6.

[9] J. Schirmer, Beyond the random-phase approximation: A new approximation scheme for the polarization propagator, Phys. Rev. A. 26 (1982) 2395–2416. doi:10.1103/PhysRevA.26.2395.

[10] M. Petersilka, U. Gossmann, E. Gross, Excitation Energies from Time-Dependent Density-Functional Theory, Phys. Rev. Lett. 76 (1996) 1212–1215. doi:10.1103/PhysRevLett.76.1212.

[11] D. Jacquemin, E.A. Perpète, I. Ciofini, C. Adamo, R. Valero, Y. Zhao, et al., On the Performances of the M06 Family of Density Functionals for Electronic Excitation Energies, J. Chem. Theory Comput. 6 (2010) 2071–2085. doi:10.1021/ct100119e.

[12] V. Barone, ed., Computational strategies for spectroscopy: from small molecules to nano systems, Wiley, Hoboken, N.J, 2012.

[13] C. Adamo, D. Jacquemin, The calculations of excited-state properties with Time-Dependent Density Functional Theory, Chem. Soc. Rev. 42 (2013) 845. doi:10.1039/c2cs35394f.

[14] J. Tomasi, B. Mennucci, R. Cammi, Quantum Mechanical Continuum Solvation Models, Chem. Rev. 105 (2005) 2999–3094. doi:10.1021/cr9904009.

[15] G. Scalmani, M.J. Frisch, B. Mennucci, J. Tomasi, R. Cammi, V. Barone, Geometries and properties of excited states in the gas phase and in solution: Theory and application of a time-dependent density functional theory polarizable continuum model, J. Chem. Phys. 124 (2006) 094107. doi:10.1063/1.2173258.

[16] O.A. Syzgantseva, V. Tognetti, L. Joubert, A. Boulangé, P.A. Peixoto, S. Leleu, et al., Electronic Excitations in Epicocconone Analogues: TDDFT Methodological Assessment Guided by Experiment, J. Phys. Chem. A. 116 (2012) 8634–8643. doi:10.1021/jp305269y.

[17] S. Chibani, A.D. Laurent, A. Blondel, B. Mennucci, D. Jacquemin, Excited-State Geometries of Solvated Molecules: Going Beyond the Linear-Response Polarizable Continuum Model, J. Chem. Theory Comput. 10 (2014) 1848–1851. doi:10.1021/ct5001507.

[18] J.P. Cerón-Carrasco, M. Fanuel, A. Charaf-Eddin, D. Jacquemin, Interplay between solvent models and predicted optical spectra: A TD-DFT study of 7-OH-coumarin, Chem. Phys. Lett.

556 (2013) 122–126. doi:10.1016/j.cplett.2012.11.075.
[19] F. De Angelis, S. Fantacci, R. Gebauer, Simulating Dye-Sensitized TiO_2 Heterointerfaces in Explicit Solvent: Absorption Spectra, Energy Levels, and Dye Desorption, J. Phys. Chem. Lett. 2 (2011) 813–817. doi:10.1021/jz200191u.
[20] D.H. Douma, B. M'Passi-Mabiala, R. Gebauer, Optical properties of an organic dye from time-dependent density functional theory with explicit solvent: The case of alizarin, J. Chem. Phys. 137 (2012) 154314. doi:10.1063/1.4758877.
[21] F. De Angelis, S. Fantacci, A. Selloni, M.K. Nazeeruddin, M. Grätzel, First-Principles Modeling of the Adsorption Geometry and Electronic Structure of Ru(II) Dyes on Extended TiO_2 Substrates for Dye-Sensitized Solar Cell Applications, J. Phys. Chem. C. 114 (2010) 6054–6061. doi:10.1021/jp911663k.
[22] V. Barone, R. Improta, N. Rega, Quantum Mechanical Computations and Spectroscopy: From Small Rigid Molecules in the Gas Phase to Large Flexible Molecules in Solution, Acc. Chem. Res. 41 (2008) 605–616. doi:10.1021/ar7002144.
[23] A. Pedone, J. Bloino, S. Monti, G. Prampolini, V. Barone, Absorption and emission UV-Vis spectra of the TRITC fluorophore molecule in solution: a quantum mechanical study, Phys. Chem. Chem. Phys. 12 (2010) 1000. doi:10.1039/b920255b.
[24] S.C.L. Kamerlin, M. Haranczyk, A. Warshel, Are Mixed Explicit/Implicit Solvation Models Reliable for Studying Phosphate Hydrolysis? A Comparative Study of Continuum, Explicit and Mixed Solvation Models, ChemPhysChem. 10 (2009) 1125–1134. doi:10.1002/cphc.200800753.
[25] I. Değirmenci, S. Eren, V. Aviyente, B. De Sterck, K. Hemelsoet, V. Van Speybroeck, et al., Modeling the Solvent Effect on the Tacticity in the Free Radical Polymerization of Methyl Methacrylate, Macromolecules. 43 (2010) 5602–5610. doi:10.1021/ma100608g.
[26] T.M. Alam, C.J. Pearce, J.E. Jenkins, Ab initio investigation of Sarin micro-hydration, Comput. Theor. Chem. 995 (2012) 24–35. doi:10.1016/j.comptc.2012.06.022.
[27] A. Le Person, A. Moncomble, J.-P. Cornard, The Complexation of Al^{III}, Pb^{II}, and Cu^{II} Metal Ions by Esculetin: A Spectroscopic and Theoretical Approach, J. Phys. Chem. A. 118 (2014) 2646–2655. doi:10.1021/jp412291z.
[28] T.C. Genaro-Mattos, Â.Q. Maurício, D. Rettori, A. Alonso, M. Hermes-Lima, Antioxidant Activity of Caffeic Acid against Iron-Induced Free Radical Generation—A Chemical Approach, PLOS ONE. 10 (2015) e0129963. doi:10.1371/journal.pone.0129963.
[29] J.P. Cornard, C. Lapouge, Theoretical and Spectroscopic Investigations of a Complex of Al(III) with Caffeic Acid, J. Phys. Chem. A. 108 (2004) 4470–4478. doi:10.1021/jp0379188.
[30] J.-P. Cornard, C. Lapouge, Absorption Spectra of Caffeic Acid, Caffeate and Their 1:1 Complex with Al(III): Density Functional Theory and Time-Dependent Density Functional Theory Investigations, J. Phys. Chem. A. 110 (2006) 7159–7166. doi:10.1021/jp060147y.
[31] M.J. Frisch, G.W. Trucks, H.B. Schlegel, G.E. Scuseria, M.A. Robb, J.R. Cheeseman, et al., Gaussian 09, Gaussian, Inc., Wallingford, CT, USA, 2009.
[32] A.D. Becke, Density-functional exchange-energy approximation with correct asymptotic behavior, Phys. Rev. A. 38 (1988) 3098–3100. doi:10.1103/PhysRevA.38.3098.
[33] C. Lee, W. Yang, R.G. Parr, Development of the Colle-Salvetti correlation-energy formula into a functional of the electron density, Phys. Rev. B. 37 (1988) 785–789. doi:10.1103/PhysRevB.37.785.
[34] S.H. Vosko, L. Wilk, M. Nusair, Accurate spin-dependent electron liquid correlation energies for local spin density calculations: a critical analysis, Can. J. Phys. 58 (1980) 1200–1211. doi:10.1139/p80-159.
[35] A.D. Becke, Density-functional thermochemistry. III. The role of exact exchange, J. Chem. Phys. 98 (1993) 5648. doi:10.1063/1.464913.
[36] W.J. Hehre, Self—Consistent Molecular Orbital Methods. XII. Further Extensions of Gaussian

—Type Basis Sets for Use in Molecular Orbital Studies of Organic Molecules, J. Chem. Phys. 56 (1972) 2257. doi:10.1063/1.1677527.
[37] P.C. Hariharan, J.A. Pople, The influence of polarization functions on molecular orbital hydrogenation energies, Theor. Chim. Acta. 28 (1973) 213–222. doi:10.1007/BF00533485.
[38] T. Clark, J. Chandrasekhar, G.W. Spitznagel, P.V.R. Schleyer, Efficient diffuse function-augmented basis sets for anion calculations. III. The 3-21+G basis set for first-row elements, Li-F, J. Comput. Chem. 4 (1983) 294–301. doi:10.1002/jcc.540040303.
[39] M. Cossi, G. Scalmani, N. Rega, V. Barone, New developments in the polarizable continuum model for quantum mechanical and classical calculations on molecules in solution, J. Chem. Phys. 117 (2002) 43. doi:10.1063/1.1480445.
[40] R.F.W. Bader, Atoms in molecules: a quantum theory, Clarendon Press ; Oxford University Press, Oxford [England] : New York, 1994.
[41] T.A. Keith, AIMAll 14.06.21, TK Gristmill Software, Overland Park, 2014.
[42] M. Palusiak, T.M. Krygowski, Application of AIM Parameters at Ring Critical Points for Estimation of π-Electron Delocalization in Six-Membered Aromatic and Quasi-Aromatic Rings, Chem. - Eur. J. 13 (2007) 7996–8006. doi:10.1002/chem.200700250.
[43] J. Poater, X. Fradera, M. Duran, M. Solà, An Insight into the Local Aromaticities of Polycyclic Aromatic Hydrocarbons and Fullerenes, Chem. - Eur. J. 9 (2003) 1113–1122. doi:10.1002/chem.200390128.
[44] J.-P. Cornard, C. Lapouge, E. André, pH influence on the complexation site of Al(III) with protocatechuic acid. A spectroscopic and theoretical approach, Spectrochim. Acta. A. Mol. Biomol. Spectrosc. 108 (2013) 280–287. doi:10.1016/j.saa.2013.02.005.
[45] R. Bianchi, G. Gervasio, D. Marabello, Experimental Electron Density Analysis of $Mn_2(CO)_{10}$: Metal−Metal and Metal−Ligand Bond Characterization, Inorg. Chem. 39 (2000) 2360–2366. doi:10.1021/ic991316e.
[46] M. Ziółkowski, S.J. Grabowski, J. Leszczynski, Cooperativity in Hydrogen-Bonded Interactions: Ab Initio and “Atoms in Molecules” Analyses, J. Phys. Chem. A. 110 (2006) 6514–6521. doi:10.1021/jp060537k.
[47] R.F.W. Bader, M.E. Stephens, Spatial localization of the electronic pair and number distributions in molecules, J. Am. Chem. Soc. 97 (1975) 7391–7399. doi:10.1021/ja00859a001.
[48] X. Fradera, M.A. Austen, R.F.W. Bader, The Lewis Model and Beyond, J. Phys. Chem. A. 103 (1999) 304–314. doi:10.1021/jp983362q.
[49] W.R. Wadt, P.J. Hay, Ab initio effective core potentials for molecular calculations. Potentials for main group elements Na to Bi, J. Chem. Phys. 82 (1985) 284. doi:10.1063/1.448800.
[50] P. Politzer, Comparison of Two Atomic Charge Definitions, as Applied to the Hydrogen Fluoride Molecule, J. Chem. Phys. 55 (1971) 5135. doi:10.1063/1.1675638.

Figure 1: Structure of caffeic acid (CA) and its complex with aluminum (CA-Al). The numbering used on CA will be used throughout.

Figure 2: Optimized structures for CA-Al (models **2** and **4**). For the sake of clarity, only the oxygen atoms of methanol in model **4** are depicted.

Figure 3: Measured UV-vis spectrum of CA-Al in methanol (from ref. [29]) and computed transitions for each of the six models for CA-Al. Some weak transitions (oscillators strengths below 0.05) have been omitted for **3'** and **4'**, located at wavelengths higher than 1000 nm.

Figure 1:

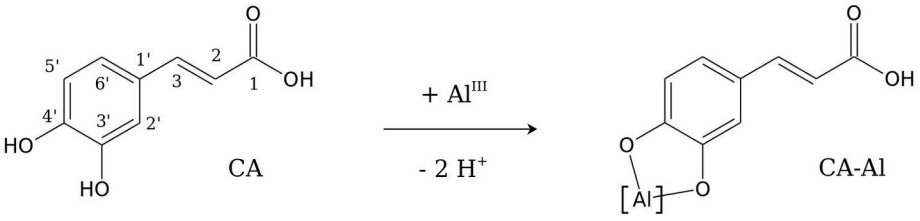

Figure 2:

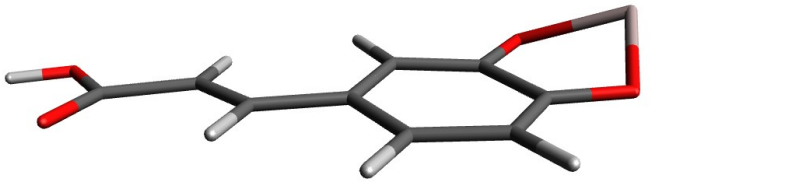

2

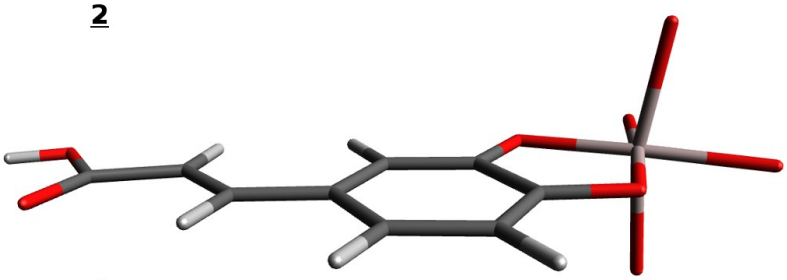

4

Figure 3:

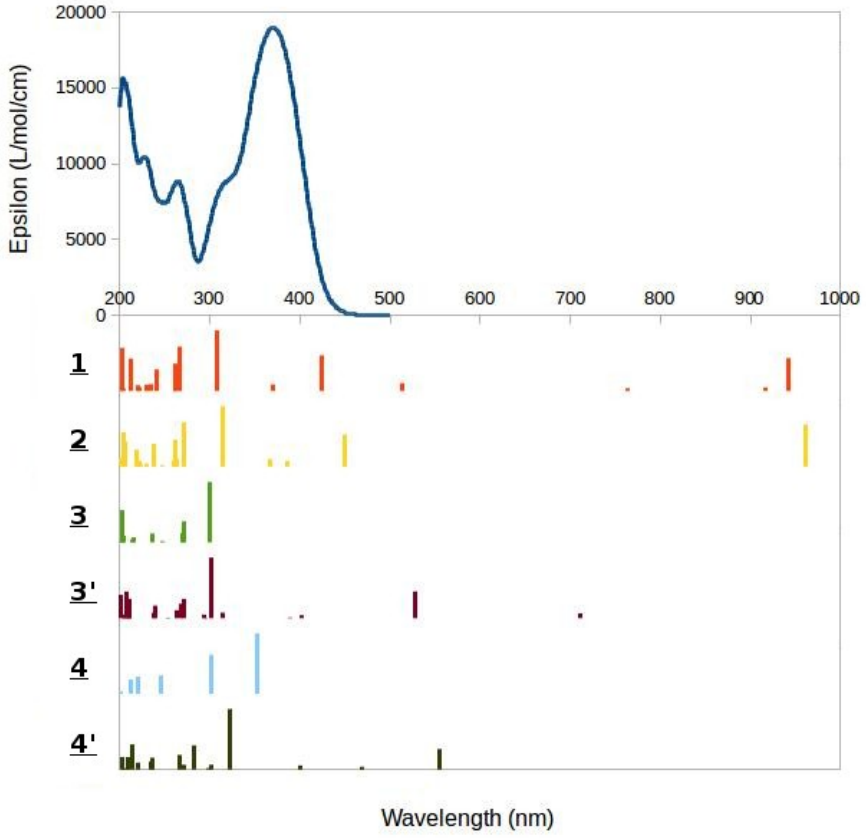
Epsilon (L/mol/cm)
20000
15000
10000
5000
0
200
300
400
500
600
700
800
900
1000
1
2
3
3'
4
4'
Wavelength (nm)

Table 1: Main characteristics of the models introduced for the study of the solvation (Y and N mean yes and no, respectively)

Model	Explicit molecules?	Continuum?	Energetic minimum?
1	N	N	Y
2	N	Y	Y
3	Y	N	Y
4	Y	Y	Y
3'	N	N	N, obtained from **3**
4'	N	Y	N, obtained from **4**

Table 2: Main geometrical parameters (bonds lengths are given in Å, angles and dihedral angles are given in degrees for CA and CA-Al), standard deviation of the six C—C bonds lengths of the benzene ring (σ_{CC}, in Å), electron density (ρ) and total electronic energy density (H) at its RCP (in Atomic Units) and Para Delocalization Index for this ring (PDI, in Atomic Units) for CA and CA-Al using models **1** to **4**.

Models	CA	CA-2H	**1**	**2**	**3** and **3'**	**4** and **4'**
Bonds						
C3'—O3'	1.369	1.283	1.304	1.306	1.374	1.354
C4'—O4'	1.357	1.267	1.285	1.292	1.377	1.350
O3'—Al	–	–	1.877	1.866	1.794	1.820
O4'—Al	–	–	1.923	1.895	1.799	1.826
Al—MeOH*	–	–	–	–	2.007	1.980
C3'—C4'	1.414	1.514	1.485	1.480	1.420	1.430
C2'—C3'	1.384	1.409	1.394	1.396	1.384	1.384
C1'—C2'	1.414	1.435	1.396	1.392	1.413	1.418
C4'—C5'	1.393	1.443	1.423	1.418	1.390	1.394
C5'—C6'	1.393	1.381	1.365	1.366	1.397	1.396
C6'—C1'	1.406	1.423	1.463	1.457	1.406	1.408
C1'—C3	1.455	1.416	1.446	1.451	1.461	1.452
C3—C2	1.350	1.388	1.354	1.350	1.345	1.353
C2—C1	1.468	1.427	1.493	1.484	1.476	1.464
C1=O	1.222	1.240	1.212	1.217	1.216	1.224
C1—O	1.358	1.386	1.341	1.345	1.358	1.360
C1O—H	0.972	0.971	0.974	0.973	0.972	0.972
Angles						
C4'-O4'-Al	–	–	109.0	108.2	107.4	109.1
C3'-O3'-Al	–	–	110.3	109.0	107.9	109.3
O3'-Al-O4'	–	–	84.2	85.5	93.3	90.6
C3'-C4'-O4'	120.1	120.9	114.7	114.8	115.9	115.6
C4'-C3'-O3'	114.3**	119.3	113.8	114.1	115.5	115.3
C1'-C3-C2	128.1	129.0	126.5	126.2	127.9	128.3
C3-C2-C1	120.3	121.5	119.0	119.8	119.8	120.4
C2-C1=O	126.5	128.6	123.8	125.0	126.0	126.8
C2-C1-OH	111.6	112.8	110.9	111.1	111.3	111.7
O=C1-OH	121.9	118.6	125.3	123.9	122.6	121.5
Dihedrals						
Al-O3'-C3'-C4'	–	–	-19.4	-20.0	-0.2	0.8
Al-O4'-C4'-C3'	–	–	19.6	20.1	0.4	-0.7
O3'-C3'-C4'-O4'	0.0	0.0	-0.6	-0.4	-0.2	-0.1
C2'-C1'-C3-C2	0.1	0.0	3.2	4.3	-0.3	0.2
C1'-C3-C2-C1	180.0	-180.0	-179.7	-179.8	-179.9	-180.0
C3-C2-C1-OH	179.9	179.9	-180.0	-179.7	180.0	-180.0
Aromaticity						

σ_{CC}	1.1	4.1	4.2	3.9	1.3	1.6
ρ(RCP)	0.0195	0.0176	0.0185	0.0187	0.0195	0.0193
H(RCP)	0.00875	0.00764	0.00820	0.00829	0.00868	0.00855
PDI	0.076	0.033	0.038	0.040	0.074	0.070

* related to **3** and **4** only, a mean value is given for these four lengths

** this value should be explained by a hydrogen bond between O3' and the H bearded by O4'

Table 3: Main electronic transitions (oscillator strengths above 0.05) computed for CA-Al using six models (given in nm (eV)) and their oscillator strengths.

Exp.	**1**		**2**		**3**		**3'**		**4**		**4'**	
λ	λ	f	λ	f	λ	f	λ	f	λ	f	λ	f
370	942.8	0.141	962.0	0.207	300.4	0.489	527.4	0.168	352.8	0.505	554.8	0.159
(3.35)	(1.32)		(1.29)		(4.13)		(2.35)		(3.51)		(2.23)	
311	423.6	0.153	449.4	0.158	271.7	0.170	302.1	0.383	301.5	0.325	323.0	0.467
(3.99)	(2.93)		(2.76)		(4.56)		(4.11)		(4.11)		(3.84)	
263	307.9	0.259	315.1	0.297	269.8	0.076	270.6	0.122	246.4	0.153	282.0	0.187
(4.71)	(0.26)		(3.94)		(4.59)		(4.58)		(5.03)		(4.40)	
225	266.6	0.190	271.0	0.218	237.6	0.073	267.7	0.091	220.8	0.144	266.2	0.113
(5.51)	(4.65)		(4.57)		(5.24)		(4.63)		(5.62)		(4.66)	
214	260.9	0.117	262.4	0.133	204.0	0.053	262.6	0.051	211.8	0.119	237.0	0.091
(5.79)	(4.75)		(4.73)		(6.08)		(4.72)		(5.86)		(5.23)	
203	241.8	0.092	238.3	0.113	202.9	0.260	239.6	0.079			234.7	0.061
(6.11)	(5.13)		(5.20)		(6.11)		(5.17)				(5.28)	
	213.1	0.139	219.2	0.083			210.3	0.123			220.6	0.054
	(5.82)		(5.66)				(5.90)				(5.62)	
	202.2	0.184	206.5	0.125			207.6	0.167			213.7	0.195
	(6.13)		(6.00)				(5.97)				(5.80)	
			204.2	0.170			201.3	0.147			208.9	0.096
			(6.07)				(6.16)				(5.94)	
											202.8	0.097
											(6.11)	

Table 4: Main electronic transitions (oscillator strengths above 0.05) computed for CA-Al using three hybrid models (given in nm (eV)) and their oscillator strengths.

Exp.	Explicit MeOH Implicit MeOH		Explicit H_2O Implicit MeOH		Explicit H_2O Implicit H_2O	
λ	λ	f	λ	f	λ	f
370 (3.35)	352.8 (3.51)	0.505	352.5 (3.52)	0.498	354.4 (3.50)	0.496
311 (3.99)	301.5 (4.11)	0.325	301.5 (4.11)	0.317	302.5 (4.10)	0.321
263 (4.71)	246.4 (5.03)	0.153	246.0 (5.04)	0.149	246.2 (5.04)	0.150
225 (5.51)	220.8 (5.62)	0.144	220.2 (5.63)	0.150	220.4 (5.63)	0.145
214 (5.79)	211.8 (5.86)	0.119	211.6 (5.86)	0.108	211.9 (5.85)	0.105
203 (6.11)						

Table 5: AIM charge of aluminum and catechol and solvent oxygen atoms, and electron density, laplacian of the electron density, kinetic electronic energy density (G), total electronic energy density (H) (in Atomic Units), opposite of the ratio between G and potential energy density (V) at the BCP and delocalization indexes (δ) for bonds involving Al in CA-Al using models **2**, **4** and the variation of **4** with water molecules.

Model	**2**	**4**	**4** with water molecules
	No explicit solvent	Explicit MeOH	Explicit H_2O
	Implicit MeOH	Implicit MeOH	Implicit MeOH
AIM charges			
Al	1.50	2.57	2.57
O3'	-1.27	-1.36	-1.36
O4'	-1.25	-1.35	-1.35
O solvent (mean)	–	-1.23	-1.26
Al—O3' bond			
ρ(BCP)	0.069	0.079	0.080
Δρ(BCP)	0.451	0.577	0.593
G(BCP)	0.1108	0.1403	0.1441
H(BCP)	0.0019	0.0039	0.0041
-G(BCP)/V(BCP)	1.02	1.03	1.03
δ(Al,O3')	0.444	0.213	0.218
Al—O4' bond			
ρ(BCP)	0.065	0.078	0.079
Δρ(BCP)	0.397	0.563	0.577
G(BCP)	0.0987	0.1371	0.1403
H(BCP)	0.0006	0.0038	0.0040
-G(BCP)/V(BCP)	1.01	1.03	1.03
δ(Al,O3')	0.445	0.211	0.213
Al—O (solvent) (mean)			
ρ(BCP)	–	0.048	0.048
Δρ(BCP)	–	0.301	0.309
G(BCP)	–	0.0717	0.0726
H(BCP)	–	0.0035	0.0047
-G(BCP)/V(BCP)	–	1.05	1.07
δ(Al,O3')	–	0.128	0.123